Global Change Biology

Global Change Biology (2016), doi: 10.1111/gcb.13451

TECHNICAL ADVANCE

Informing climate models with rapid chamber measurements of forest carbon uptake

DANIEL B. METCALFE[1], DANIEL RICCIUTO[2], SARI PALMROTH[3], CATHERINE CAMPBELL[4], VAUGHAN HURRY[4], JIAFU MAO[2], SONJA G. KEEL[5], SUNE LINDER[6], XIAOYING SHI[2], TORGNY NÄSHOLM[4,7], KLAS E. A. OHLSSON[7], M. BLACKBURN[7], PETER E. THORNTON[2] and RAM OREN[3]

[1]*Department of Physical Geography and Ecosystem Science, Lund University, Lund SE-223 62, Sweden,* [2]*Environmental Sciences Division, Climate Change Science Institute, Oak Ridge National Laboratory, Oak Ridge, TN 37831-6335, USA,* [3]*Nicholas School of the Environment, Duke University, Durham, NC 27708-0328, USA,* [4]*Department of Forest Genetics and Plant Physiology, Umeå Plant Science Centre, Swedish University of Agricultural Sciences, Umeå SE-901 83, Sweden,* [5]*Institute for Sustainability Sciences, Agroscope, Zurich 8046, Switzerland,* [6]*Southern Swedish Forest Research Centre, Swedish University of Agricultural Sciences, Alnarp SE-230 53, Sweden,* [7]*Department of Forest Ecology and Management, Swedish University of Agricultural Sciences, Umeå SE-901 83, Sweden*

Abstract

Models predicting ecosystem carbon dioxide (CO_2) exchange under future climate change rely on relatively few real-world tests of their assumptions and outputs. Here, we demonstrate a rapid and cost-effective method to estimate CO_2 exchange from intact vegetation patches under varying atmospheric CO_2 concentrations. We find that net ecosystem CO_2 uptake (NEE) in a boreal forest rose linearly by 4.7 ± 0.2% of the current ambient rate for every 10 ppm CO_2 increase, with no detectable influence of foliar biomass, season, or nitrogen (N) fertilization. The lack of any clear short-term NEE response to fertilization in such an N-limited system is inconsistent with the instantaneous downregulation of photosynthesis formalized in many global models. Incorporating an alternative mechanism with considerable empirical support – diversion of excess carbon to storage compounds – into an existing earth system model brings the model output into closer agreement with our field measurements. A global simulation incorporating this modified model reduces a long-standing mismatch between the modeled and observed seasonal amplitude of atmospheric CO_2. Wider application of this chamber approach would provide critical data needed to further improve modeled projections of biosphere–atmosphere CO_2 exchange in a changing climate.

Keywords: boreal forest, earth system model, model-data integration, nutrient limitation, photosynthetic downregulation, *Pinus sylvestris*

Received 19 February 2016; revised version received 20 June 2016 and accepted 23 July 2016

Introduction

The terrestrial biosphere has the potential to either accelerate or slow the pace of the rise in global atmospheric CO_2 concentrations (Kirtman *et al.*, 2013), with major implications for the frequency and magnitude of detrimental climate change impacts (Friedlingstein *et al.*, 2006). Therefore, accurate predictions from earth system models (ESMs) about the spatial extent and temporal development of terrestrial ecosystem CO_2 responses are urgently required to inform climate adaptation and mitigation strategies. While free-air CO_2 enrichment (FACE) experiments provide crucial information in this respect (Kimball *et al.*, 2002; Long *et al.*, 2004; Ainsworth & Long, 2005; Norby & Zak, 2011), two critical knowledge gaps remain, both relating to the general lack of replication of FACE studies due to their logistical complexity and high financial cost: first, the interactive effects of multiple environmental factors on ecosystem CO_2 responses, and second, the variability of CO_2 responses among plant functional groups and across major global biomes, particularly high-latitude and tropical systems that play central roles in global climate but remain critically undersampled by FACE studies (Hickler *et al.*, 2008; Leakey *et al.*, 2012 but see Norby *et al.*, 2016). This means that both the direct and indirect (via interactions with other factors) effects of rising atmospheric CO_2 across large areas of the world are currently inferred by extrapolating beyond the range of available data.

Experimental manipulations, ecosystem observations, and process modeling all suggest that the components of net ecosystem exchange (NEE) of CO_2

Correspondence: Daniel B. Metcalfe, tel. +46 72 2052795, fax +46 46 2220321, e-mail: dbmetcalfe@gmail.com

© 2016 John Wiley & Sons Ltd

(photosynthetic gains, and respiration and other losses) are controlled in part by the availability of mineral nutrients and that nutrient limitation is a common condition in many biomes (Fisher *et al.*, 2012). However, observations at different spatial scales provide a complex and sometimes puzzling picture of the nature and degree of influence of nutrient availability on NEE. Photosynthetic rates assessed at the cellular and leaf scales are often higher than the observed accumulation of carbon (C) in plant and soil pools measured at the whole ecosystem level would suggest, after accounting for well-understood losses due to respiration and disturbance processes (Bonan *et al.*, 2011). This discrepancy suggests that C uptake and plant growth become uncoupled under conditions of nutrient limitation, Several downregulation mechanisms that might account for this uncoupling have been proposed, some with partial empirical support (Fisher *et al.*, 2010), but many ESMs choose to instantly downregulate photosynthesis with increasing atmospheric CO_2 under conditions of soil N limitation (Thornton *et al.*, 2007). This means that most ESMs predict, for the large portion of the terrestrial biosphere limited by soil nutrients, only weak stimulation of CO_2 uptake (and NEE) over short timescales by increasing CO_2. Long-term CO_2 enrichment studies suggest a more progressive, rather than instantaneous, mechanism for nitrogen (N) limitation (Luo *et al.*, 2004), but a clear means to rigorously assess competing downregulating mechanisms is lacking.

In this study, we describe an approach to fill this, and potentially other, important gaps in our current scientific understanding of ecosystem CO_2 responses with a relatively simple, fast and cost-effective method for quantifying the instantaneous responses of net ecosystem exchange of CO_2 (NEE_i) within intact ecosystems to changes in atmospheric CO_2. We ask whether and how the sensitivity of whole-forest NEE_i to variation in atmospheric CO_2 at the site changes (i) over 250 to 550 ppm in ambient atmospheric CO_2, and (ii) across plot differences in vegetation structure (tree stem basal area and foliar mass), seasonal growth stage, and/or soil N availability. Further, we used the results to constrain simulations of ecosystem CO_2 uptake within a major ESM (Community Land Model 4.5) (Oleson *et al.*, 2013), by testing model output against observed plot NEE_i at 400 ppm (NEE_{400}) and the slope of change in NEE_i with atmospheric CO_2. Specifically, we use the chamber data to improve model representation of one important but poorly constrained process – the underlying basis for the widely observed excess C uptake capacity in steady-state systems (Bonan *et al.*, 2011) – and demonstrate the wider effects of including this novel constraint on the simulated seasonal cycle of atmospheric CO_2 at a global scale.

Materials and methods

Study site and experimental design

The experiment was conducted in a ~14-year-old, naturally regenerating boreal *Pinus sylvestris* L. forest at Rosinedalsheden (64°09′N, 19°05′E, 145 m above sea level) in northern Sweden. The site has a sparse understory of dwarf shrubs, *Calluna vulgaris* L. and *Vaccinium vitis idaea* L., and a ground layer of *Cladonia* spp. lichens. The soil is podzolic, with a 2- to 3-cm-thick organic mor layer, a C : N ratio of 33 : 1, and pH (in H_2O) of 4.5. Eight forest plots (50 m^2) were sealed within an airtight 4-m-tall chamber made of clear, gas impermeable polyurethane plastic stretched over an aluminum frame on largely cloudless days in the growing season of 2007, and 25 l of $^{13}CO_2$ were injected into the chamber to raise internal CO_2 concentrations up to 160 ppm above ambient levels of 395 ppm (Table 1, Fig. 1). Then, the CO_2 concentrations (together with ambient air temperature and relative humidity) within the sealed chambers under clear sky conditions were recorded with infrared gas analyzers (IRGAs) (EGM-4, PP Systems, Amesbury, MA, USA; GMP343, Vaisala, Vantaa, Finland). Outside the period of CO_2 measurements (<3 h Fig. 4a), plots were completely open to the atmosphere. As a first

Table 1 Summary of plot characteristics. Data represent values from each plot (50 m^2 area). Data on tree age, height, and basal area do not include stems <1.3 m height. Tree age and height values represent plot means. Soil respiration values represent means from 16 to 25 repeated measurements over 10 days since labeling from 3 points per plot. Tree foliar N represents means of current year needles samples from five trees per plot. Plots with the prefix C and N denote Control and N-fertilized plots respectively. Plots 1–2 and 3–4 were first surveyed (and fertilized if N plots) in June and August 2007, respectively

	C1	N1	C2	N2	C3	N3	C4	N4
Tree number	51	49	103	97	47	44	44	59
Tree age (years)	14	14	12	11	11	12	14	13
Tree height (m)	2.9	3.3	2.3	2.4	1.9	1.8	2.6	2.5
Tree basal area (cm^2)	384	476	138	182	129	185	366	357
Understory mass (kg)	12.5	10.7	11.5	14.6	12.0	11.9	10.2	15.7
Tree foliar N (g m^{-2})	0.6	0.7	0.6	0.8	1.0	1.0	1.3	1.8
Soil respiration (g CO_2 m^{-2} h^{-1})	0.12	0.20	0.16	0.23	0.32	0.20	0.26	0.51

Fig. 1 The chambers in operation at the study site (photograph courtesy of M. Blackburn).

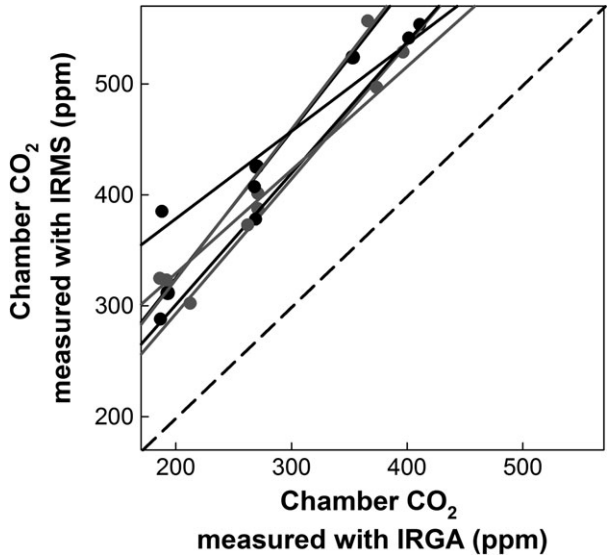

Fig. 2 Relationship between chamber CO_2 concentrations measured with infrared gas analyzers and isotope ratio mass spectrometer. Circles and lines denote measurements and the regression fits to measurements, respectively. Gray = control plots, black = fertilized plots. The dashed line represents the 1 : 1 line.

assessment of potential interactions between NEE_i responses to atmospheric CO_2 concentrations and other environmental factors, we made these measurements at different points during the summer growing season in 2007 and fertilized four of the eight plots with N two weeks prior to measurements. During the period of chamber CO_2 measurement, the chambers were sealed to the ground with chains while an air conditioner within the chamber maintained air temperature near ambient levels and air humidity below saturating levels, while also mixing the chamber air at a rate of 400 m^3 min^{-1} (entire chamber air volume cycled every 30 s).

Measurements

Immediately after sealing each chamber, 25 l of pure CO_2 was injected with >96 atom percent ^{13}C (Spectra Gases, Alpha, NJ, USA). Commercial IRGAs are tuned to detect $^{12}CO_2$ rather than $^{13}CO_2$, so the raw uptake curves measured with the IRGA underestimated the true total CO_2 concentration ($^{12}CO_2$ and $^{13}CO_2$) within the chamber. To correct for this, samples of chamber gas were taken at the beginning, middle, and end of the period of chamber enclosure and submitted to an isotope ratio mass spectrometer (IRMS ANCA TG system, 20-20 analyzer, Europa Scientific Ltd, Crewe, UK) to measure the actual total CO_2 concentration over time in each chamber. We related chamber CO_2 concentrations measured at the same points in time from both the IRGAs and IRMS (Fig. 2). The linear relation between IRGA-measured and actual CO_2 concentration measured by IRMS for each plot ($R^2 = 0.97 \pm 0.01$) was applied to each plot IRGA-measured CO_2 uptake curve, to derive corrected CO_2 uptake curves.

These corrected curves of CO_2 concentration change with time since chamber enclosure were quality-checked to remove periods when clouds passed overhead (9% of total data) which were identified from abrupt changes in the otherwise smooth, gradual decline in chamber CO_2 concentrations, as respiratory fluxes continued but photosynthetic CO_2 uptake was suppressed. The resulting 'cleaned' curves, which isolate the effects of atmospheric CO_2 on NEE_i, form the basis for the main analysis (Fig. 4a). To attribute NEE_i to as specific an ambient CO_2 concentration as possible, NEE_i was calculated from CO_2 change every 30 s within every chamber. However, over such narrow time windows the CO_2 changes were often at the limit of the IRGA measurement resolution (PP Systems: 1 ppm, Vaisala: 0.005 ppm), so we fitted a three-parameter decay model to each cleaned curve to estimate CO_2 for any point in time given the pattern of CO_2 change over the entire measurement duration:

$$y = a + b \times \exp^{-c \times t}$$

where y represents the predicted chamber CO_2 concentration (ppm), a, b, and c represent the three fitted curve parameters and t refers to the time (minutes) since measurements began after chamber enclosure. Across all plots, there was a close agreement between cleaned, measured data and fitted curves (Fig. 3). All plots were a net sink of CO_2 at the time of measurements (Fig. 4a), so the decline in chamber CO_2 concentrations from initial levels down to a minimum of ~250 ppm below ambient levels was used to simulate historic and potential future atmospheric CO_2 levels. The measured rate of decline in CO_2 concentrations after the chamber was sealed was used to calculate NEE_i in the early and late growing season (Fig. 4b). NEE_i (g CO_2 m^{-2} h^{-1}) was calculated as:

$$\mathrm{NEE}_i = \frac{\Delta c}{\Delta t} \times \frac{p}{RT} \times \frac{V}{A} \times \mathrm{M}_{\mathrm{CO}_2} \times 3.6 \cdot 10^{-3}$$

where $\Delta c/\Delta t$ represents the change in atmospheric CO_2 concentrations (ppm) over time (seconds) when the chamber was sealed, p is atmospheric pressure (Pa), T is the temperature of air (K), V is the internal volume of the chamber (m^3), and A is the ground area (m^2) covered by the chamber. The value M_{CO2}

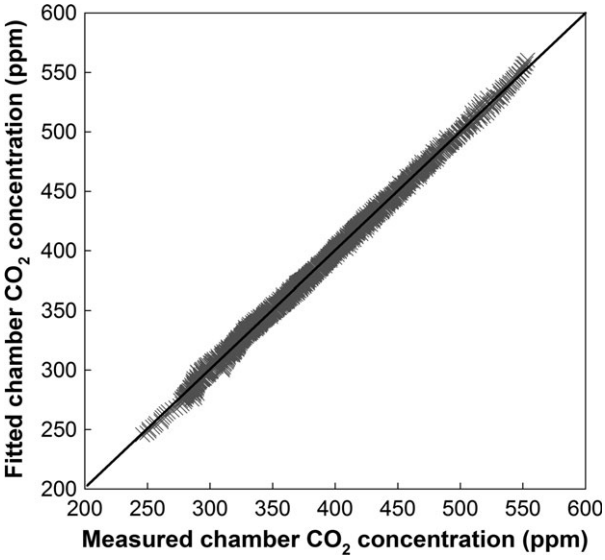

Fig. 3 Relationship between modeled and measured chamber CO_2 concentrations, for all plots (gray crosses). Overcast periods were removed from measured data (9% of total data). The black line denotes the 1 : 1 ratio. The root mean-squared error between fitted and measured data is 2.28, and the r^2 of a linear regression through the data is 0.999.

represents the molar mass of CO_2 (44.01 g mol^{-1}), and R denotes the universal gas constant (8.31 J mol^{-1} K^{-1}). Both p and T were recorded concurrently with CO_2 measurements by the IRGAs installed inside each chamber. For each plot, mean NEE_i was estimated for 10 ppm bins between 250 and 550 ppm. Modeled changes in soil CO_2 efflux due to altered chamber CO_2 concentrations were performed with the method of Ohlsson (2011), using measured soil respiration rates (Subke *et al.*, 2009) and chamber CO_2 concentrations.

Over the brief period of enclosure within the chamber, we assume that changes in respiration from nonphotosynthetic aboveground plant tissue due to altered chamber CO_2 concentrations were negligible. A site-parameterized soil CO_2 transport model (Ohlsson, 2011) was used to quantify, and correct for, changes in soil CO_2 efflux caused by altered chamber CO_2 concentration. The patterns of NEE_i observed therefore represent responses of net photosynthesis to variation in atmospheric CO_2 concentrations. Leaf-level measurements demonstrate near-instantaneous responses of stomata and net photosynthesis to changes in ambient atmospheric CO_2 concentrations (Jach & Ceulemans, 2000; Leakey *et al.*, 2006) so we relate NEE_i to chamber CO_2 concentrations recorded over the same time period. In both the early and late growing seasons of 2007, two of the plots were fertilized with a single dose of 100 kg N ha^{-1} two weeks prior to measurements for comparison with two matching unmodified control plots to assess seasonal and immediate N fertilization effects.

Model simulations

To evaluate the potential for the chamber measurements to constrain key ESM processes, simulations were performed at

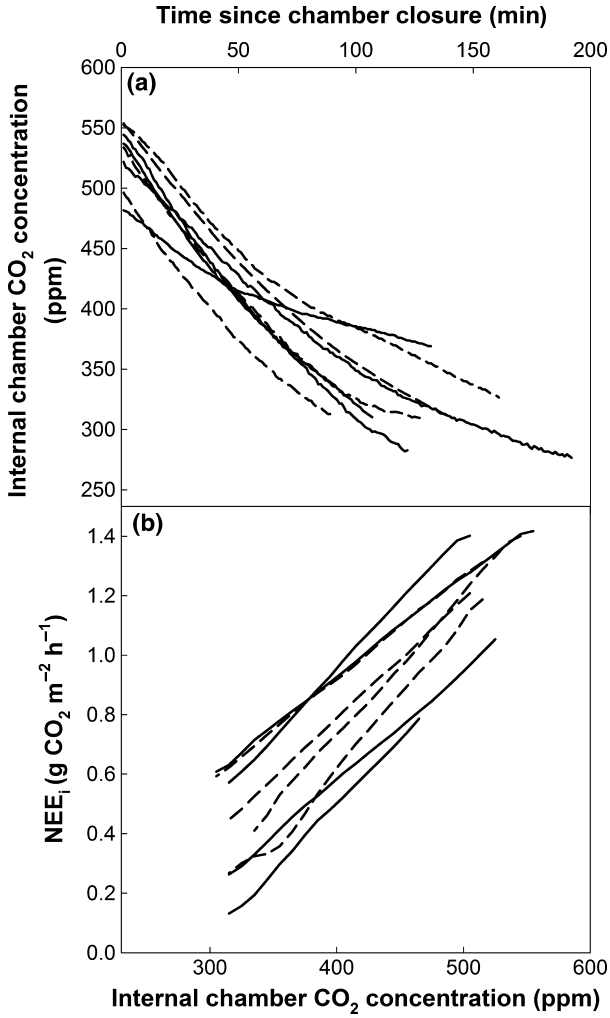

Fig. 4 Shifts in CO_2 concentration and CO_2 uptake rate over time after sealing the chambers. (a) Declining CO_2 concentrations after chamber closure indicates net ecosystem CO_2 uptake or positive NEE_i. The slope of the decline in CO_2 concentrations for a given CO_2 concentration window yielded (b) NEE_i estimates over the range of CO_2 concentrations recorded within each chamber. Solid and dashed lines denote fertilized and unfertilized plots, respectively.

the experimental site with the Community Land Model version 4.5 (Oleson *et al.*, 2013) with C and N cycling (henceforth referred to as CLM 4.5CN) using observed meteorology, vegetation, and soil physical properties. We performed simulations with the default version of the model, and with a new version that enables carbohydrate storage (described below). For both model versions, 1000-year simulations were conducted using pre-industrial N deposition and atmospheric CO_2 concentrations to achieve steady-state C fluxes and pools. Starting in the year 1850, transient atmospheric CO_2 concentrations, N and aerosol deposition, and land use change forcings were applied, including a harvest in the year 1996 in the site simulations to produce a forest of the same age as the study site. A half-hourly model timestep was used through 2006. To resolve

the uptake curves in the site simulations, a 10-min model timestep was used in the years 2007–2008. To simulate the experimental manipulation, simulated net ecosystem productivity was used to draw down atmospheric CO_2 concentrations using the appropriate chamber volumes on the days of the experiments. Photosynthetically active radiation (PAR) was held constant during the simulated experiment. We did not attempt to simulate the observed variability among plots, so all model experiments used the same initial conditions in the year 2007. When applied directly to the soil mineral N pool as deposition to simulate study site N fertilization, the fertilizer disappears completely within several days because of the one-day turnover associated with 'bulk denitrification' in CLM 4.5CN. Therefore, N fertilization was not applied directly as deposition but instead was simulated in CLM 4.5CN assuming no N limitation (in CLM terms, 'carbon-only' mode) after the date of fertilization for the duration of the growing season.

The revised model assumes that rather than instantaneous downregulation of gross primary productivity (GPP) as in the default model, the excess C flux (C that cannot be allocated due to insufficient N supply) is stored as nonstructural carbohydrates (NSCs) in a new pool. While CLM 4.5CN already contains storage pools, the allocation of C and N to these existing pools is constrained by stoichiometry of vegetation components with the exception of reserve pools to satisfy growth and maintenance respiration demands when GPP is insufficient (Oleson *et al.*, 2013). Additionally, the stoichiometrically constrained storage pools are only active in deciduous systems, and therefore not relevant for the experimental site. Carbon is allocated to the new NSC pool for all vegetation types when N supply is insufficient for instantaneous allocation to structural pools after growth and maintenance respiration demands are satisfied. While this modification does not affect the structural biomass, the instantaneous GPP is generally higher and the total biomass is increased by the magnitude of NSCs held in reserve. Carbon in the simulated NSC pool is initially assumed to return to the atmosphere with a 1-year turnover time. In reality, the fate of NSCs is much more complicated than this simplistic representation; some is likely to be held as starches and sugars with residence times from years to decades (Richardson *et al.*, 2013), while others are used in more rapidly in metabolism or root exudation (Högberg *et al.*, 2010; Keel *et al.*, 2012). We then explore the sensitivity of the results to this turnover parameter, which represents an aggregation of several different processes. For simplicity, NSCs are not allocated to other plant or soil pools, and NSC turnover to the atmosphere is included as a single additional respiration term.

To explore some broader implications of this modification within CLM 4.5CN, we performed multiple fully coupled climate–biogeochemistry simulations with the CESM1 model (including either the default or the revised versions of the CLM 4.5CN land submodel), using historical fossil fuel, land use, and N deposition forcings to bring the model forward from 1850 to 1999. Because our simplistic modification does not affect biomass or net C fluxes on long timescales, the same initial conditions may be used for both model versions. An existing set of initial conditions beginning in the year 1980 from the default model was used for both simulations, eliminating the need for costly model spinup. Simulations were run for 20 years. We assume that with a 1-year NSC turnover time, model drift associated with the transient 'filling' of NSC pool in the modified model is negligible over 10 years after initialization from the default model. The second 10-year period in the simulations was then used to evaluate the seasonal cycle of predicted atmospheric CO_2 concentrations. We evaluated the predicted seasonal cycle of atmospheric CO_2 concentrations against the GlobalView analysis of observed marine concentrations (NOAA Greenhouse Gas Marine Boundary Layer Reference at http://www.esrl.noaa.gov/gmd/ccgg/mbl/data.php) for the final decade of simulation. Atmospheric CO_2 is sampled from the Community Atmosphere Model (CAM) output at the lowest vertical level.

Statistical analysis

Mean differences in the slope of change in NEE_i with rising CO_2 concentration relative to NEE_i at ambient CO_2 concentration, grouped by fertilization treatment and season ($n = 2$), were analyzed with a univariate ANOVA. Variables were log-transformed where necessary, to conform to the assumptions of parametric statistical analysis. Associations between the slope of change in NEE_i with rising CO_2 concentration relative to NEE_i at ambient CO_2 concentration and key stand properties (tree basal area and foliar mass, understory vegetation cover, soil CO_2 efflux) were assessed with a nonparametric Spearman's rank correlation. Analyses were conducted with SPSS-PASW STATISTICS 18 software (IBM Corporation, Armonk, NY, USA).

Results

To control for variation in absolute NEE_i among plots, we quantified NEE_i at different CO_2 concentrations as a proportion of the rate of NEE_i at current ambient CO_2 concentration (~400 ppm) for each plot. From these standardized slope data, NEE_i increased linearly over the entire recorded CO_2 range across all forest plots sampled, by a mean rate (± standard error) of 4.7 ± 0.2% from current ambient rates for every 10 ppm increase (Fig. 5a). The near linearity of this response is broadly consistent with leaf-level observations over the same CO_2 concentration span (Wullschleger, 1993; Manter & Kerrigan, 2004). The relative response of NEE_i to CO_2 was well conserved across plots (Fig. 5a), despite considerable interplot variation in soil N status, seasonal growth status, and stand structure (Table 1). Thus, across 308% and 370% variation in foliar N mass and stem basal area among plots, there was only 139% variation in the slopes describing the relative increase in NEE_i with atmospheric CO_2 concentrations. The N fertilization treatment had increased mean current year needle N concentration by 26.6 ± 5.9% when NEE_i measurements commenced yet

there were no significant effects either of fertilization two weeks prior (ANOVA: df = 1, F = 4.184, P = 0.87), or of the timing of measurements in the growing season (ANOVA: df = 1, F = 3.02, P = 0.60) on relative NEE_i change with atmospheric CO_2 concentrations. Basic stand properties, such as tree basal area, foliar mass, understory vegetation cover, and soil CO_2 efflux, were not significantly correlated with observed interplot variation in relative NEE_i sensitivity to atmospheric CO_2 concentrations. These results are tentative given the limited plot replication, although power analysis demonstrates that the level of treatment replication (n = 2) was sufficient to detect a change (~ 37%) comparable to the observed shifts in foliar N (26.6 ± 5.9%) or foliar mass (67.7 ± 22.6%) associated with the fertilization and season plot groupings, respectively.

This observed invariant relative NEE_i response to CO_2 contrasts with the more variable, and nonlinear, relative NEE_i responses to CO_2 simulated by the default CLM 4.5CN model (Figs 5b and 6a). Specifically, the model predicts that relative NEE_i is more responsive to atmospheric CO_2 after N fertilization (Fig. 5b) and at low levels of ambient atmospheric CO_2, when the instantaneous downregulation is lower (Fig. 6a). This discrepancy between observations and CLM 4.5CN predictions was substantially reduced by removing the default instantaneous downregulation mechanism within CLM 4.5CN and adding instead a temporary nonstructural carbohydrate (NSC) storage pool with a 1-year turnover time (Fig. 5c). The remaining nonlinearity in the modeled NEE_i response to CO_2 is related to increasing stomatal resistance as CO_2 concentrations decrease. This nonlinearity does not appear in the observations, implying that the model predictions of stomatal conductance are incorrect. This may be related to an equilibration time slower than the model timestep of 10 min, although instantaneous responses are likely (Leakey *et al.*, 2006). However, around 400 ppm, the predicted stomatal resistance does not change rapidly and the slope is nearly linear, supporting the model-data comparison in Fig. 6a.

The seasonal amplitude of atmospheric CO_2 concentrations is one of the key metrics in several multimodel intercomparison projects and is consistently underestimated by most ESMs (including CESM1) (Zhao & Zeng, 2014; Peng *et al.*, 2015). The simple revision to the CLM 4.5CN submodel including a NSC storage pool with a 1-year turnover time, prompted by and tested against empirical data, significantly improved model representation of the global mean seasonal cycle amplitude for atmospheric CO_2 concentrations without affecting other aspects of the simulation (Fig. 6b). Model revision raised estimated global terrestrial GPP by around 23%, but did not affect NPP as the additional assimilate was diverted to autotrophic respiration. Assuming NSC storage turnover >1 year had no effect on simulated seasonal cycle amplitude of atmospheric CO_2 concentrations. Overall, this result further supports the

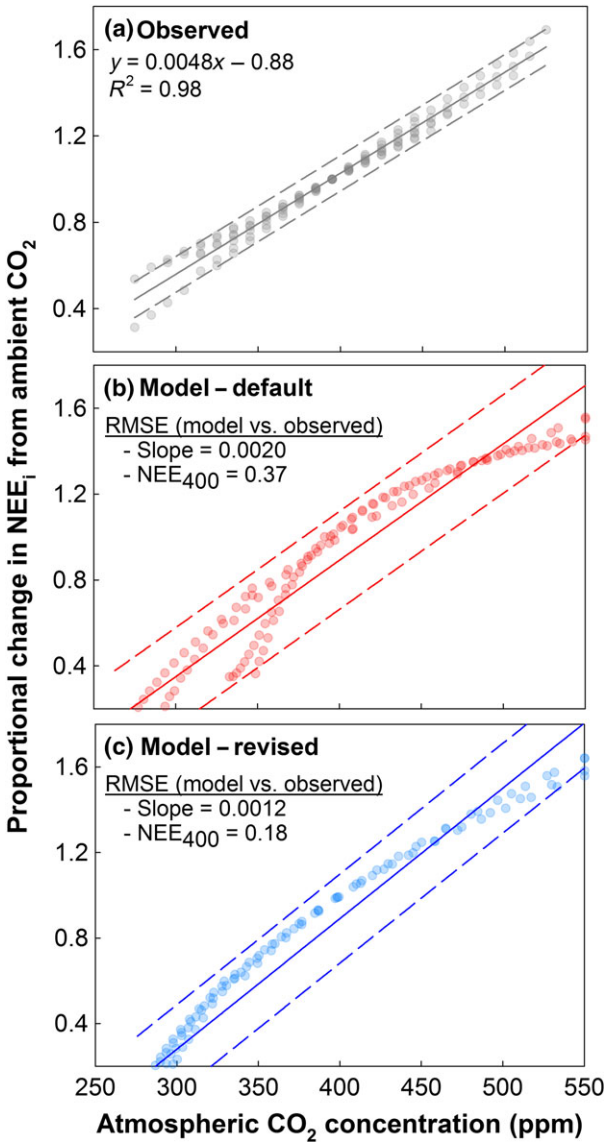

Fig. 5 The measured and modeled change in relative NEE_i with ambient atmospheric CO_2 concentrations at the study plots. (a) field observations, (b) the default CLM 4.5CN model with instant photosynthetic downregulation and no C storage mechanism and (c) a modified CLM 4.5CN model where excess photosynthetic C is channeled to a carbohydrate storage pool. The separate RMSE values for slope and NEE_{400} refer to the fit between modeled and observed data between the slope of change in NEE_i with CO_2 and NEE_i at the CO_2 concentration of 400 ppm on each plot, respectively. In all panels, dots denote plot data, while solid lines are linear regression fits through the data and the dashed lines indicate 95% prediction intervals around the regressed means.

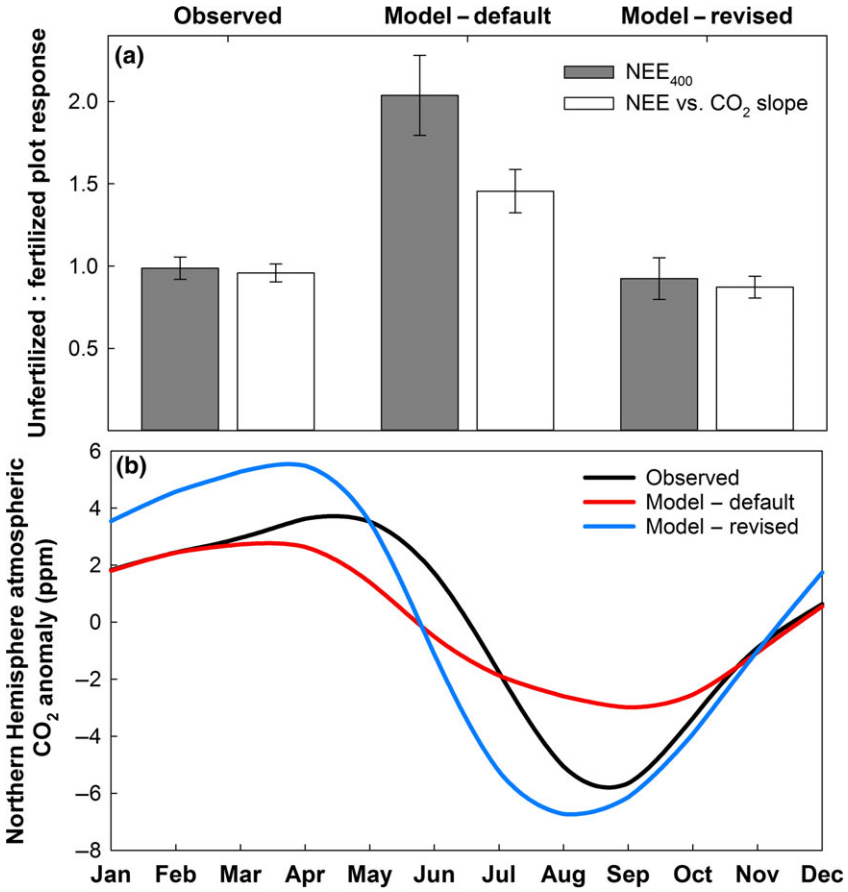

Fig. 6 Comparison of default and revised model estimates of key local and global parameters. (a) The relative difference between fertilized and unfertilized study plots in terms of NEE_{400} and the slope of the change in NEE_i with ambient CO_2 concentrations according to observations, the default (without C storage) and the modified (with C storage) CLM 4.5CN model. Slope and NEE_{400} refers to the fit between modeled and observed data between the slope of change in NEE_i with CO_2 and NEE_i at the CO_2 concentration of 400 ppm on each plot, respectively. The bars and errors represent plot means and standard errors (n = 8). (b) The seasonal anomaly in Northern Hemisphere atmospheric CO_2 concentrations according to observations, the default (without C storage) and the modified (with C storage) CLM 4.5CN model incorporated into the CESM1 ESM. The seasonal atmospheric CO_2 cycle is presented as an anomaly from the 1992 to 1999 detrended signal. Observations come from marine boundary layer data from NOAA ESRL.

conclusion that instantaneous downregulation as represented in many current ESMs is unrealistic (Thornton *et al.*, 2007), and demonstrates the need for improved modeling of C storage and allocation to capture both short-term and long-term C cycle responses. Further work, refining model GPP estimates, the extent of N downregulation, allocation to structural C, and longer-term mechanisms of downregulation following N limitation (e.g., shifts in C : N ratios) could further improve our modeled estimate of the seasonal cycle in atmospheric CO_2.

Discussion

Large chambers such as those featured in this study have long been used to record ecosystem CO_2 fluxes (e.g., Rosenthal *et al.*, 1999; Arnone & Obrist, 2003). Here, we illustrate a novel application of these chambers, to assess the short-term CO_2 sensitivity of NEE and test ESM representations of ecosystem functioning. The study suggests that N is not limiting NEE at sub-daily timescales, despite strong evidence that the study system is highly N-limited over annual timescales (Högberg *et al.*, 2010; Keel *et al.*, 2012). The assumption of instantaneous NEE downregulation, formalized in many global ESMs (Thornton *et al.*, 2007), is therefore inconsistent with the experimental data at this site (Figs 5a and 6a), suggesting that a more complex mechanism is required to explain the fate of photosynthate that cannot be allocated to structural tissues because of insufficient soil N availability. Our explanation that a significant portion of excess assimilated C is allocated to NSC with longer turnover results in improved agreement between model predictions and observations and

is consistent with site measurements showing rapid transfer of recent photosynthetic assimilate to roots and turnover of starch in root material >80 days (Keel *et al.*, 2012). More broadly, models that account for multiple NSC pools better compare with observed isotopic ^{14}C and woody increment data than models that do not include NSC (Richardson *et al.*, 2013).

The chambers can be erected by two people within half a day with simple tools and easily available, commercial scaffolding frameworks. A small, light-weight crane/forklift truck is required to carry the chamber plastic and air conditioning system to the site. As such, installation causes minimal disturbance to the surrounding environment and may take place some distance away from forest edges or roads. As the measurements themselves take only a few hours, replicate plot measurements of NEE_i sensitivity to CO_2 may be collected within 1–2 days using this method. Start-up costs of the system are around US$50 000 for chamber frame and plastic fabrication, the air conditioner, IRGA, and other sensors. Ongoing costs associated with vehicle rental and fuel costs and scaffolding rental amount to around ~US$2000 per week, although these could be removed almost entirely for long-term projects by purchasing these equipments instead of renting them. Including an additional 10% for system maintenance costs, we therefore estimate that annual operation of this chamber would cost approximately US $170 000, equivalent to around 5% of the mean budget for construction and annual operation of a typical FACE facility (Reichle, 2002). During this period, assuming conservatively that one measurement can be taken every two days, it would be possible to collect around 130 replicate measurements of NEE_i response to CO_2 variation per year. Critical constraints to this sampling efficiency are the frequency of long cloud-free periods during days throughout the year, and the geographical location and scale of the planned sampling. Biomes with frequent cloud cover could still be adequately sampled by investing in more than one chamber to intensively ample during cloud-free periods, and cutting on ongoing maintenance and rental costs. Additional time and financial costs associated with equipment transport in remote areas or across disparate study plots would also clearly be incurred.

Together with the complementary information gathered from FACE experiments, open-top and whole-tree chambers, and ongoing experimentation with smaller-scale approaches, the ecosystem chamber method outlined here provides a valuable new avenue for future research that would significantly improve our ability to understand and predict the trajectory of land net ecosystem C exchange in a changing climate. These instantaneous chamber measurements cannot resolve some major questions, such as the long-term fate of assimilated C and the extent of photosynthetic acclimation to CO_2 concentrations and these issues are best addressed by FACE studies (Kimball *et al.*, 2002; Long *et al.*, 2004; Ainsworth & Long, 2005; Norby & Zak, 2011). Yet the chamber approach outlined here nevertheless potentially provides useful information about long-term responses because: (i) Short-term differences in plant ecophysiology and C processing within the plant can scale up to long-term changes in ecosystem biogeochemistry and atmospheric CO_2 (Jarvis & McNaughton, 1985; Raupach, 1995; Cramer *et al.*, 1999); and (ii) while the CO_2 responses themselves are transitory in the approach outlined here, how these responses interact with other factors can be examined under conditions closer to steady state than are possible within FACE experiments. For example, FACE experiments have made important contributions in understanding whether and how ecosystem CO_2 fertilization might be limited by other conditions, most notably soil N availability which has been modified through addition of fertilizer (Luo *et al.*, 2004). A problem with these findings is that the observations then reflect the responses of a system still transitioning from abrupt, step changes in not just one, but two key resources (CO_2 and soil N) which may be different to system responses to gradual shifts in the same resources (e.g., Gundersen & Wullschleger, 1994). In the case of non-steady-state responses to CO_2, some insights may be provided from ecosystems around naturally occurring CO_2 springs but these conditions are rare (Paoletti *et al.*, 2005). However in the case of soil N and many other potentially important limiting factors (site temperature, moisture, stand age), this source of uncertainty could be effectively addressed through chamber measurements of NEE_i sensitivity to CO_2 along natural gradients in these factors where the ecosystems sampled have equilibrated to the factor in question (Walker *et al.*, 2010).

Given the relative ease, speed and low costs associated with this approach, it can be easily reproduced by many scientific groups, and widely replicated across multiple ecosystems and land use types, and within multifactorial matrices of different treatments to examine the kind of complex interactions that are currently poorly represented within ESMs. The chambers can be easily installed over short stature vegetation (<5 m height), which accounts for a large portion of terrestrial vegetation particularly in arid systems (Cao & Woodward, 1998; Simard *et al.*, 2011) but is relatively understudied and appears to play a key role in global climate (Poulter *et al.*, 2014). Application of the chamber approach in higher stature vegetation will incur significant additional analytical and logistical complications

and financial costs, although the same is likely true for FACE studies (Lapola & Norby, 2014). Most critically, with increasing chamber volume, maintaining constant air temperature and humidity and adequately mixing the air would require significant modifications to the air conditioning system. While these additional challenges will negatively alter the cost–benefit ratio of the chamber approach, they could still be installed in taller vegetation at a small fraction of the cost and time of a typical FACE experiment. Looking to what can be done in the near future to address critical knowledge gaps currently constraining ESM predictions of biosphere–atmosphere interactions, we argue that the best approach will be to invest in relatively fast and cost-effective methods, such as the one outlined in this study to constrain specific ESM components and processes under a range of conditions and ecosystem types.

Acknowledgements

The work was supported by the Kempe Foundations, the Swedish Science Council (VR), the Swedish Research Council for Environment, Agricultural Sciences and Spatial Planning (Formas), and the Swedish University of Agricultural Sciences. The manuscript benefitted from the unwavering support and profound insights of P. Högberg and M. Högberg. We thank Henrik Holmgren for access to his land, and Jan Parsby, Thomas Hörnlund, and Stephan Schaffner for technical assistance. We are also grateful to colleagues from York (Phil Ineson, Jens-Arne Subke and Harry Vallack) for field help. This material is based upon work supported by the U.S. Department of Energy, Office of Science, Office of Biological and Environmental Research, and conducted as part of the Accelerated Climate Modeling for Energy (ACME) project and the Oak Ridge National Laboratory Terrestrial Ecosystem Science Focus Area project. This research used resources of the Oak Ridge Leadership Computing Facility at the Oak Ridge National Laboratory, which is supported by the Office of Science of the U.S. Department of Energy under Contract No. DE-AC05-00OR22725.

References

Ainsworth EA, Long SP (2005) What have we learned from 15 years of free-air CO_2 enrichment (FACE)? A meta-analytic review of the responses of photosynthesis, canopy properties and plant production to rising CO_2. *New Phytologist*, **165**, 351–371.

Arnone JA III, Obrist DA (2003) Large daylight geodesic dome for quantification of whole-ecosystem CO_2 and water vapour fluxes in arid shrublands. *Journal of Arid Environments*, **55**, 629–643.

Bonan GB, Lawrence PJ, Oleson KW *et al.* (2011) Improving canopy processes in the Community Land Model version 4 (CLM4) using global flux fields empirically inferred from FLUXNET data. *Journal of Geophysical Research*, **116**, G02014.

Cao M, Woodward FI (1998) Net primary and ecosystem production and carbon stocks of terrestrial ecosystems and their responses to climate change. *Global Change Biology*, **4**, 185–198.

Cramer W, Kicklighter DW, Bondeau A *et al.* (1999) Comparing global models of terrestrial net primary productivity (NPP): overview and key results. *Global Change Biology*, **5**, 1–15.

Fisher JB, Sitch S, Malhi Y, Fisher RA, Huntingford C, Tan S-Y (2010) Carbon cost of plant nitrogen acquisition: a mechanistic, globally applicable model of plant nitrogen uptake, retranslocation, and fixation. *Global Biogeochemical Cycles*, **24**, GB1014.

Fisher JB, Badgley G, Blyth E (2012) Global nutrient limitation in terrestrial vegetation. *Global Biogeochemical Cycles*, **26**, GB3007.

Friedlingstein P, Cox P, Betts R *et al.* (2006) Climate-carbon cycle feedback analysis: results from the C4MIP model intercomparison. *Journal of Climate*, **19**, 3337–3353.

Gundersen CA, Wullschleger SD (1994) Photosynthetic acclimation in trees to rising atmospheric CO_2: a broader perspective. *Photosynthesis Research*, **39**, 369–388.

Hickler T, Smith B, Prentice IA, Mjöfors K, Miller P, Arneth A, Sykes MT (2008) CO_2 fertilization in temperate FACE experiments not representative of boreal and tropical forests. *Global Change Biology*, **14**, 1531–1542.

Högberg MN, Briones MJ, Keel SG *et al.* (2010) Quantification of effects of season and nitrogen supply on tree below-ground carbon transfer to ectomycorrhizal fungi and other soil organisms in a boreal pine forest. *New Phytologist*, **187**, 485–493.

Jach ME, Ceulemans R (2000) Effects of season, needle age and elevated atmospheric CO_2 on photosynthesis in Scots pine (*Pinus sylvestris*). *Tree Physiology*, **20**, 145–157.

Jarvis PG, McNaughton KG (1985) Stomatal control of transpiration: scaling up from leaf to region. *Advances in Ecological Research*, **15**, 1–49.

Keel SG, Campbell CD, Högberg MN *et al.* (2012) Allocation of carbon to fine root compounds and their residence times in a boreal forest depend on root size class and season. *New Phytologist*, **194**, 972–981.

Kimball BA, Kobayashi K, Bindi M (2002) Responses of agricultural crops to free-air CO_2 enrichment. *Advances in Agronomy*, **77**, 293–368.

Kirtman B, Power SB, Adedoyin JA *et al.* (2013) Near-term climate change: projections and predictability. In: *Climate Change 2013: The Physical Science Basis. Contribution of Working Group I to the Fifth Assessment Report of the Intergovernmental Panel on Climate Change* (eds Stocker TF, Qin D, Plattner G-K, Tignor M, Allen SK, Boschung J, Nauels A, Xia Y, Bex V, Midgley PM), pp. 953–1008. Cambridge University Press, Cambridge.

Lapola DM, Norby RJ (2014) Amazon-FACE: Assessing the effects of increased atmospheric CO_2 on the ecology and resilience of the Amazon forest – Science Plan and Implementation Strategy. Ministry of Science, Technology and Science, Brasilia, Brazil.

Leakey ADB, Bernacchi CJ, Ort DR, Long SP (2006) Long-term growth of soybean at elevated [CO_2] does not cause acclimation of stomatal conductance under fully open-air conditions. *Plant, Cell and Environment*, **29**, 1794–1800.

Leakey ADB, Bishop KA, Ainsworth EA (2012) A multi-biome gap in understanding of crop and ecosystem responses to elevated CO_2. *Current Opinion in Plant Biology*, **15**, 228–236.

Long SP, Ainsworth EA, Rogers A, Ort DR (2004) Rising atmospheric carbon dioxide: plants FACE the future. *Annual Review of Plant Biology*, **55**, 591–628.

Luo Y, Su B, Currie WS *et al.* (2004) Progressive nitrogen limitation of ecosystem responses to rising atmospheric carbon dioxide. *BioScience*, **54**, 731–739.

Manter DK, Kerrigan J (2004) A/C_i curve analysis across a range of woody plant species: influence of regression analysis parameters and mesophyll conductance. *Journal of Experimental Botany*, **55**, 2581–2588.

Norby RJ, Zak DR (2011) Ecological lessons from free-air CO_2 enrichment (FACE) experiments. *Annual Review of Ecology, Evolution and Systematics*, **42**, 181–203.

Norby RJ, De Kauwe MG, Domingues TF *et al.* (2016) Model–data synthesis for the next generation of forest free-air CO_2 enrichment (FACE) experiments. *New Phytologist*, **209**, 17–28.

Ohlsson KEA (2011) Theoretical model of the abiotic component of soil ^{13}CO2 tracer efflux in ^{13}C pulse-labeling experiments on plant-soil systems. *Soil Biology and Biochemistry*, **43**, 675–681.

Oleson KW, Lawrence DM, Bonan GB *et al.* (2013) *Technical Description of version 4.5 of the Community Land Model (CLM)*. Ncar Technical Note NCAR/TN-503+STR, National Center for Atmospheric Research, Boulder, CO.

Paoletti E, Pfanz H, Raschi A (2005) Pros and cons of CO_2 springs as experimental sites. In: *Plant Responses to Air Pollution and Global Change* (eds Omasa K, Nouchi I, de Kok LJ), pp. 195–202. Springer Verlag, Tokyo.

Peng S, Ciais P, Chevallier F *et al.* (2015) Benchmarking the seasonal cycle of CO_2 fluxes simulated by terrestrial ecosystem models. *Global Biogeochemical Cycles*, **29**, 46–64.

Poulter B, Frank D, Ciais P *et al.* (2014) Contribution of semi-arid ecosystems to interannual variability of the global carbon cycle. *Nature*, **509**, 600–603.

Raupach MR (1995) Vegetation–atmosphere interaction and surface conductance at leaf, canopy and regional scales. *Agricultural and Forest Meteorology*, **73**, 151–180.

Reichle D (2002) An Evaluation of the Department of Energy's Free-Air Carbon Dioxide Enrichment (FACE) Experiments as Scientific User Facilities. U.S. Department of Energy, Washington DC, USA.

Richardson AD, Carbone MS, Keenan TF *et al.* (2013) Seasonal dynamics and age of stemwood nonstructural carbohydrates in temperate forest trees. *New Phytologist*, **197**, 850–861.

Rosenthal Y, Farnsworth B, Rodrigo Romo FV, Lin G, Marino BDV (1999) High quality, continuous measurements of CO_2 in Biosphere 2 to assess whole mesocosm carbon cycling. *Ecological Engineering*, **13**, 249–262.

Simard M, Pinto N, Fisher JB, Baccini A (2011) Mapping forest canopy height globally with spaceborne lidar. *Journal of Biogeochemical Research: Biogeosciences*, **116**, G4.

Subke J-A, Vallack HW, Magnusson T, Keel SG, Metcalfe DB, Högberg P, Ineson P (2009) Short-term dynamics of abiotic and biotic soil $^{13}CO_2$ effluxes after in situ $^{13}CO_2$ pulse labelling of a boreal pine forest. *New Phytologist*, **183**, 349–357.

Thornton PE, Lamarque JF, Rosenbloom NA, Mahowald NM (2007) Influence of carbon–nitrogen cycle coupling on land model response to CO_2 fertilization and climate variability. *Global Biogeochemical Cycles*, **21**, GB40182007.

Walker LR, Wardle DA, Bardgett RD, Clarkson BD (2010) The use of chronosequences in studies of ecological succession and soil development. *Journal of Ecology*, **98**, 725–736.

Wullschleger SD (1993) Biochemical limitations to carbon assimilation in C_3 plants – a retrospective analysis of the A/C_i curves from 109 species. *Journal of Experimental Botany*, **44**, 907–920.

Zhao F, Zeng N (2014) Continued increase in atmospheric CO_2 seasonal amplitude in the 21st century projected by the CMIP5 Earth system models. *Earth System Dynamics*, **5**, 423–439.